Inhibitors

International Edition: DOI: 10.1002/anie.201905578
German Edition: DOI: 10.1002/ange.201905578

Discovery of a Potent GLUT Inhibitor from a Library of Rapafucins by Using 3D Microarrays

*Zufeng Guo[+], Zhiqiang Cheng[+], Jingxin Wang[+], Wukun Liu, Hanjing Peng, Yuefan Wang, A. V. Subba Rao, Ruo-jing Li, Xue Ying, Preethi Korangath, Maria V. Liberti, Yingjun Li, Yongmei Xie, Sam Y. Hong, Cordelia Schiene-Fischer, Gunter Fischer, Jason W. Locasale, Saraswati Sukumar, Heng Zhu, and Jun O. Liu**

Abstract: *Glucose transporters play an essential role in cancer cell proliferation and survival and have been pursued as promising cancer drug targets. Using microarrays of a library of new macrocycles known as rapafucins, which were inspired by the natural product rapamycin, we screened for new inhibitors of GLUT1. We identified multiple hits from the rapafucin 3D microarray and confirmed one hit as a bona fide GLUT1 ligand, which we named rapaglutin A (RgA). We demonstrate that RgA is a potent inhibitor of GLUT1 as well as GLUT3 and GLUT4, with an IC_{50} value of low nanomolar for GLUT1. RgA was found to inhibit glucose uptake, leading to a decrease in cellular ATP synthesis, activation of AMP-dependent kinase, inhibition of mTOR signaling, and induction of cell-cycle arrest and apoptosis in cancer cells. Moreover, RgA was capable of inhibiting tumor xenografts in vivo without obvious side effects. RgA could thus be a new chemical tool to study GLUT function and a promising lead for developing anticancer drugs.*

Glucose is a universal cellular fuel that serves as both an energy source and a building block for a variety of macromolecules. In comparison to normal cells, cancer cells have a higher demand for glucose due to their faster proliferation rate and aerobic glycolysis as a consequence of the Warburg effect.[1] Several common cancer driver mutations such as p53 and KRAS, as well as hypoxia, have been shown to upregulate the expression of glucose transporters, prominent among which are members of the facilitative glucose transporter family including GLUT1 and GLUT3.[2] Inhibition of GLUTs has been shown to not only block cancer cell growth but also sensitize cancer cells to other drugs.[3] Extensive efforts have been made to discover new inhibitors of GLUTs, particularly GLUT1, as leads for developing novel anticancer drugs.[4] Although a number of GLUT inhibitors have been reported, including BAY-876,[5] a potent and isoform-specific GLUT1 inhibitor, none has entered the clinic to date.

We recently generated a library of macrocycles named rapafucins, that were inspired by the natural products rapamycin and FK506. The premise of the rapafucin design is to exploit the FKBP-binding domain of rapamycin and FK506 that confers favorable cellular and pharmacokinetic advantages on macrocycles and use it as a key scaffold to display non-natural oligopeptides in place of the effector domains of rapamycin and FK506. The ability of rapafucins to bind FKBP proteins to form a tight complex confers a number of advantages for drug leads, including greater stability, higher intracellular accumulation, larger size and better pharmacokinetic and pharmacodynamic properties than smaller molecules lacking the ability to bind FKBP. [6] We have designed and synthesized a 45000 compound rapafucin library and

[*] Dr. Z. Guo,[+] Dr. Z. Cheng,[+] Dr. J. Wang,[+] Dr. W. Liu, Dr. H. Peng, Dr. Y. Wang, Dr. A. V. S. Rao, Dr. R. J. Li, Dr. X. Ying, Dr. Y. Li, Dr. Y. Xie, Dr. S. Y. Hong, Prof. Dr. J. O. Liu
Department of Pharmacology and Molecular Sciences
The SJ Yan and HJ Mao Laboratory of Chemical Biology
Johns Hopkins University School of Medicine
Room 516, Hunterian Building, 725 N. Wolfe Street
Baltimore, MD (USA)
E-mail: joliu@jhu.edu

Prof. Dr. H. Zhu
Department of Pharmacology and Molecular Sciences
Johns Hopkins University School of Medicine (USA)

Dr. P. Korangath, Prof. Dr. S. Sukumar, Prof. Dr. J. O. Liu
Department of Oncology
Johns Hopkins University School of Medicine (USA)

M. V. Liberti, Prof. Dr. J. W. Locasale
Department of Pharmacology and Cancer Biology
Duke University School of Medicine (USA)

Prof. Dr. C. Schiene-Fischer, Prof. Dr. G. Fischer
Department of Enzymology
Institute for Biochemistry and Biotechnology
Martin Luther University Halle-Wittenberg (Germany)

Dr. J. Wang[+]
Current address: Department of Medicinal Chemistry
The University of Kansas, KS (USA)

Dr. W. Liu
Current address: Institute of Chinese Medicine
Nanjing University of Chinese Medicine, Nanjing (China)

Dr. R. J. Li
Current address: Food and Drug Administration
Silver Spring, MD (USA)

Dr. X. Ying
Current address: School of Pharmaceutical Sciences
Shihezi University, Shihezi (China)

Dr. Y. Xie
Current address: Cancer Center, West China Hospital
Sichuan University, Chengdu (China)

Dr. S. Y. Hong
Current address: Rapafusyn Pharmaceuticals, Baltimore, MD (USA)

[+] Authors contributed equally to this work.

Supporting information (including experimental details) and the ORCID identification number for one of the authors of this article can be found under: https://doi.org/10.1002/anie.201905578.

identified promising hits against several targets, including a potent and isoform-specific inhibitor of the human equilibrative nucleoside transporter (hENT)1 that showed in vivo efficacy in an animal model of ischemic kidney reperfusion injury.[7] Given that hENT1 and GLUT belong to the same superfamily of solute carrier transporters, we were prompted to screen the rapafucin library for new GLUT1 inhibitors. In the current study, we developed a 3D small-molecule microarray by immobilizing 3918 rapafucins on a single chip and screened cell lysates containing stably expressed GLUT1. We identified a potent inhibitor, named rapaglutin A (RgA), that inhibits GLUT1 as well as GLUT3 and GLUT4. We also demonstrated that RgA inhibits glucose uptake, induces cell apoptosis, and inhibits the growth of tumor xenografts of breast cancer cells in vivo.

Small-molecule microarrays have been shown to be a powerful platform for high-throughput screening.[8] Among the different methods of small-molecule immobilization, we chose to use pre-assembled diazirine that upon activation by UV light, generates a reactive carbene species to covalently react with and capture small molecules. As macrocycles, rapafucins are particularly suitable for this platform since multiple sites for immobilization exist around the periphery of the macrocycles. Given the stochastic nature of the carbene-mediated crosslinking reaction, there is a high probability that a fraction of a given rapafucin species will be covalently immobilized via positions that would not interfere with its binding to target protein. To develop a rapafucin microarray for high-throughput screening, we explored both 2D and 3D surface structures prefabricated on glass slides (Figure 1 a). Unlike the 2D surface structure,[9] the 3D surface structure was fabricated by growing polymers on the glass surface with each polymeric chain carrying up to hundreds of trifluoromethylphenyl diazirine moieties, thereby significantly increasing the number of sites for rapafucin immobilization on the 3D surface and at the same time providing a biocompatible environment for rapafucin–protein interactions (Figure 1 a, Figure S1 in the Supporting Information).[10]

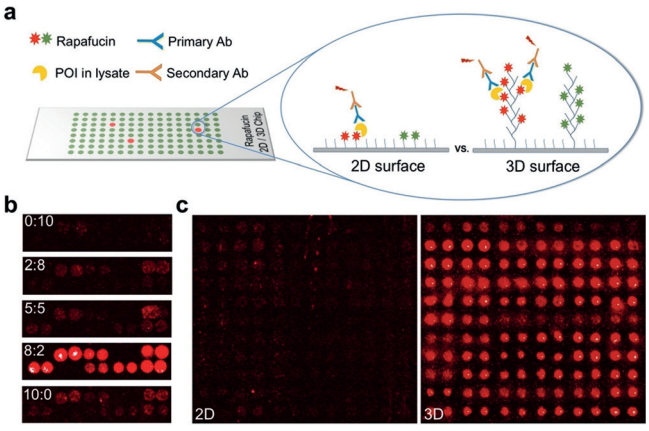

Figure 1. a) Construction of the rapafucin 2D and 3D microarrays. Ab = antibody, POI = protein of interest; red star = positive POI binder; green star = negative POI binder. b) Small-molecule array screening against purified GST-FKBP12 on a 3D copolymer diazirine surface with different ratios of monomers: PEGMA/DMAEMA = 0:10, 2:8, 5:5, 8:2 or 10:0. c) Comparison of the interaction between rapafucins and FKBP12 on 2D and 3D surfaces. Microarray images of the rapafucin 2D and 3D microarrays probed by purified GST-FKBP12. All of the compounds were spotted in duplicate.

To develop the 3D surface for the fabrication of rapafucin microarrays, we attempted to optimize the polymer density both horizontally and vertically to achieve the highest sensitivity. Horizontal density was controlled by mixing 2-bromoisobutyryl bromide and propionyl bromide (as the spacer) at different molar ratios to control the density of active atom-transfer radical polymerization (ATRP) initiation sites as previously described.[10] We applied 1:100 ratio of 2-bromoisobutyryl bromide and propionyl bromide to our 3D surface without further optimization since this ratio is commonly used to achieve high sensitivity of 3D surface.[10a,d] Vertical density was manipulated using poly-(PEGMA-co-DMAEMA) matrix to maximize the binding of proteins to adjacent ligands displayed on the same polymer. We optimized the vertical density by adjusting the gradient ratio of monomer PEGMA and DMAEMA followed by determination of binding of FKBP12 to the resultant 3D surface, since all rapafucins contain an embedded FKBP-binding domain. The highest signal-to-background ratio (SBR) was obtained at a PEGMA/DMAEMA ratio of 8:2 (Figure 1 b, Figure S2). Using this optimized diazirine-containing 3D surface grafted onto a glass slide, we robotically arrayed a rapafucin library[7] containing 3918 individual compounds to the glass. As a comparison, we also arrayed the same 3918 individual rapafucins onto a slide grafted onto a 2D surface displaying the same diazirine as previously described.[9] Once stock solutions of the rapafucin library were arrayed on the 2D or 3D surface and most of solvent carrier was evaporated, the crosslinking reaction was initiated by irradiating the surfaces with 365 nm UV light.[11] We next compared the 2D and the newly developed 3D surface for their capacity to bind FKBP12 under the same conditions, the SBR of the binding of FKBP12 on the 3D surface is on average 6-fold greater than that on the 2D surface (Figure 1 c, Figure S3), thus indicating that the 3D microarray of rapafucins is a superior platform for screening target proteins.

To screen for GLUT1-interacting rapafucins, we stably overexpressed GLUT1 in HEK293T cells and generated cell lysates containing detergent-solubilized recombinant GLUT1 (Figure S4). We next incubated the GLUT1-containing cell lysate on both 2D and 3D rapafucin microarrays. After washing the slides to remove unbound proteins, the bound GLUT1 protein was detected with anti-GLUT1 antibodies, followed by visualization with Cy5-labeled secondary antibodies using a microarray scanner. Rapafucins were scored as positive hits when the corresponding SBR was greater than 3. Based on this criterion, a total of 17 rapafucin hits and one positive control (BAY-876) were identified on the 3D rapafucin microarray. In contrast, only one hit (WL13-F11, also among the 17 hits identified from the 3D rapafucin microarray) was identified on the 2D rapafucin microarray (Table S1, Figure S5).

To determine which of the 17 rapafucin hits inhibits the transporter activity of GLUT1, we employed an orthogonal glucose uptake assay using 2-deoxy-D-[^{3}H]glucose ([^{3}H]-2DG), a nonhydrolyzable radioactive glucose analogue.

Each hit was separately incubated with A549 cells for 10 min before the amount of [^{3}H]-2DG taken up by the cells was measured using scintillation counting. Two of the 17 hits, JW11-D2 and HP17-C2 (Figure 2a and b), were found to block the uptake of [^{3}H]-2DG appreciably with IC_{50} values of 11.6 nM and 243 nM, respectively (Figure 2c, Table S1). In light of the potent inhibition of glucose uptake by JW11-D2, we named it rapaglutin A (RgA).

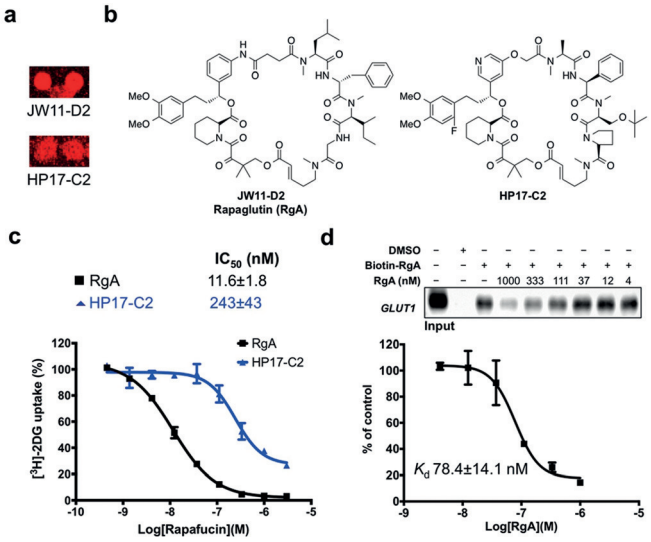

Figure 2. a) 3D Microarray images of the two positive hits for GLUT1 binding, JW11-D2 and HP17-C2. b) Chemical structures of JW11-D2 (rapaglutin A, RgA) and HP17-C2. c) Inhibition of 2-deoxy-D-[^{3}H] glucose ([^{3}H-2DG) uptake in A549 cells by RgA and HP17-C2. d) Competition profile of biotin-RgA binding to GLUT1 in HEK 293T cell lysate by RgA.

Next, we determined the binding affinity of RgA for GLUT1 using a biotin pull-down assay. We synthesized a biotin-RgA conjugate by tethering the biotin moiety through a carbon–carbon double bond in the FKBP-binding domain of RgA (Figure S6). An [^{3}H]-2DG uptake assay in A549 cells revealed that biotin-RgA retained inhibitory activity against GLUT1 with an IC_{50} value of 211 nM (Figure S6), thus suggesting that the biotin-RgA conjugate remained active against GLUT1 albeit with lower potency. Using the biotin-RgA conjugate, we performed a pull-down experiment with cell lysate containing detergent-solubilized GLUT1 protein prepared from HEK293T cells overexpressing GLUT1, followed by Western blot analysis with a GLUT1-specific antibody. The biotin-RgA conjugate was capable of pulling down GLUT1 (Figure 2d), thus further confirming that RgA directly interacts with GLUT1. Importantly, binding of GLUT1 to the biotin-RgA probe is dose-dependently competed by free RgA, thus allowing determination of the binding affinity of RgA for GLUT1 with an estimated K_d value of 78 nM (Figure 2d).

GLUT1 is a basal glucose transporter expressed in almost all cell types, and is upregulated in many cancer cells.[12] To determine whether RgA could inhibit glucose uptake in cancer cell lines in addition to A549, we measured the impact of RgA on [^{3}H]-2DG uptake in six other cancer cell lines,

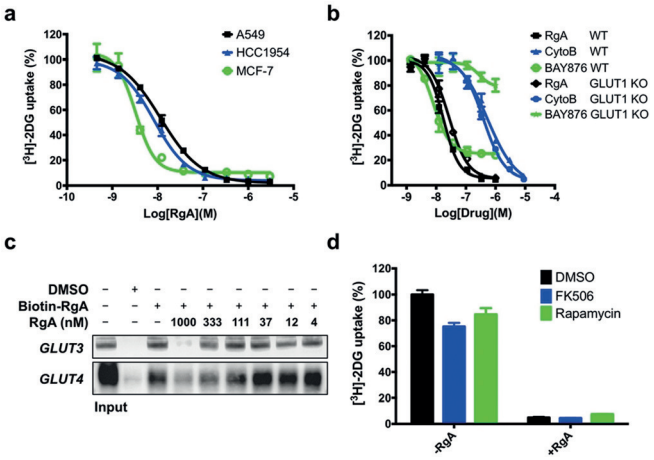

Figure 3. RgA shows isoform-nonspecific and FKBD-independent inhibition of glucose transporters. a) Inhibition of 2-deoxy-D-[^{3}H] glucose ([^{3}H]-2DG) uptake in A549, HCC1954, and MCF-7 cells by RgA. b) Inhibition of [^{3}H]-2DG uptake in DLD1 wild type or GLUT1 knock out cells by RgA, BAY-876, and Cytochalasin B (CytoB). c) Competition profiles of biotin-RgA binding to GLUT3 and GLUT4 by RgA. d) Inhibition of [^{3}H]-2DG uptake in MCF-7 cells by 100 nM of RgA, 20 μM of FK506, 20 μM of rapamycin, and combinations.

including HCC1954, MCF-7, PANC10.05, Jurkat T, HeLa, and RKO (Figure 3a, Table S2). We observed that RgA dose-dependently inhibited glucose uptake in all cell lines tested, with IC_{50} values ranging from 3 nM to 19 nM (Table S2). Among them, the breast cancer cell line MCF-7 was most sensitive to RgA, with an IC_{50} of 3.3 nM. These results demonstrated that RgA has a general inhibitory effect on glucose uptake in all cancer cell lines tested.

The human GLUT family consists of 14 members that differ in substrate affinity, specificity, and tissue distribution.[12] We determined whether RgA is specific for GLUT1 using a pair of isogenic cell lines. DLD-1 wild-type (for GLUT1) and DLD-1 *GLUT1* knock-out (for GLUT3)[5] cells were treated in parallel with RgA, BAY-876, a reported GLUT1-specific inhibitor, and cytochalasin B, a non-specific GLUT inhibitor,[13] followed by assessment of [^{3}H]-2DG uptake. As expected, BAY-876 lost its inhibitory activity but cytochalasin B maintained its inhibitory activity in *GLUT1* knock-out cells (Figure 3b). Similar to cytochalasin B, RgA inhibited glucose uptake in both wild-type and *GLUT1* knock-out cells with IC_{50} values of 17.5 nM and 27.1 nM, respectively, thus suggesting that RgA, unlike BAY-876, is not specific for GLUT1 (Figure 3b, Table S3). To further assess the isoform specificity, we overexpressed three other isoforms of glucose transporters, including GLUT2, 3, and 4, in HEK 293T *GLUT1* knock-out cells. The overexpression of GLUT2 in HEK293T cells did not succeed for unknown reasons. Using the [^{3}H]-2DG uptake assay, RgA was also found to block glucose uptake in GLUT4-overexpressing cells with an IC_{50} value of 25.9 nM (Table S4). In addition, similar to the result of GLUT1 pull-down, biotin-RgA was able to pull down both GLUT3 and GLUT4 (Figure 3c). RgA exhibited lower binding affinity against GLUT3 and GLUT4, with estimated K_d values of 330 nM and 98.2 nM, respectively (Figure 3c, Table S4). These results suggested that RgA is

a non-specific inhibitor of multiple isoforms of GLUTs, including at least GLUT1, 3, and 4.

Like FK506 and rapamycin, RgA contains an FKBP-binding domain. We determined the binding affinity of RgA for different isoforms of FKBP. Interestingly, RgA showed binding selectivity among different isoforms of FKBPs, with the highest affinity for FKBP12 ($K_i = 1.5$ nM for inhibition of the prolyl isomerase activity; Table S5). The ability of RgA to form a complex with FKBP12 raised the question of whether FKBP is required for its interaction with GLUTs. A hallmark of FKBP dependence is that the cellular effects can be antagonized by other FKBP-binding ligands with no or orthogonal biological activity, as has been shown for FK506 and rapamycin.[14] High concentrations of FK506 and rapamycin had negligible effect on the inhibitory activity of RgA in the [^{3}H]-2DG uptake assay (Figure 3d). To further determine the dependence of RgA on endogenous FKBP, we knocked out three major isoforms of FKBP (*FKBP12*, *51*, and *52*) using CRISPR-Cas9 in Jurkat T-cells.[7] Unlike the ENT1 inhibitor rapadocin,[7] knockout of the three FKBP isoforms showed negligible effect on the sensitivity of cells to RgA (Figure S7). Taken together, these results strongly suggest that the inhibitory activity of RgA is independent of endogenous FKBP.

To understand the metabolic impact of GLUT inhibition by RgA, we determined the steady-state levels of 272 metabolites using LC–MS[15] in MCF-7 cells upon treatment with RgA for 30 min and 6 h. As shown in Figure 4a, the most significant metabolic changes caused by RgA are related to glycolysis. Specifically, there were significant decreases in three upper glycolytic intermediates, including glucose-6-phosphate (G6P), fructose 1,6-bisphosphate (F1,6-BP), and dihydroxyacetone phosphate (DHAP), and three key pentose phosphate pathway intermediates, including 6-phosphogluconic acid (6PGA), ribose 5-phosphate (R5P), and erythrose-4-phosphate (E4P; Figure 4a and b). In contrast, the TCA cycle and redox status were not significantly affected by RgA treatment of MCF-7 cells ($p > 0.001$) (Figure S8). Together, these results suggest that the metabolic effects of RgA are due almost exclusively to the inhibition of glucose uptake.

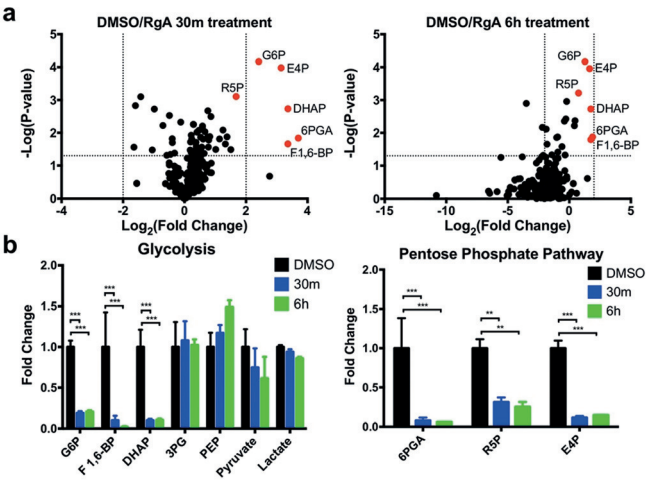

Figure 4. RgA inhibition of glycolysis. a) Volcano plots showing metabolite profiles of MCF-7 cells treated with RgA for 30 min or 6 h treatment periods compared to cells treated with vehicle (DMSO). Log2 fold change versus −log10 p value. Dotted lines along *x*-axis represent ±log2 (2) fold change and dotted line along *y*-axis represents −log10 (0.05). Metabolites ±log2 (2) fold change shown as red dots with metabolite names denoted. All other metabolites are shown as black dots. b) Upper glycolysis metabolites and pentose phosphate pathway decrease after 30 min or 6 h treatments with RgA; P value is from two-sided student t-test. *** $p < 0.0001$; ** $p < 0.001$.

A major consequence of inhibition of GLUT is a decrease in the level of cellular ATP and a corresponding increase in the AMP/ATP ratio, which was indeed observed upon treatment of MCF-7 cells with RgA (Figure S8c). The increase in the AMP/ATP ratio, in turn, is expected to activate AMPK, thereby leading to the inhibition of the mTOR signaling pathway.[3b,16] We therefore determined the effect of RgA on AMPK and mTOR activity in MCF-7 cells. RgA activated AMPK and inhibited mTOR activity in a time- and dose-dependent manner (Figure S9). These results suggest that AMPK likely acts as the key link between the upper glycolysis inhibition and subsequent mTOR-pathway inhibition.

We next determined the effects of RgA on cell growth, survival, and cell death. Cell-cycle analysis revealed that treatment of MCF-7 cells with RgA for 24 h led to G1 cell-cycle arrest (Figure S10a). In addition, 24 h treatment with RgA led to activation of both p53 and p21 in a dose-dependent manner (Figure S10b). Prolonged treatment of MCF-7 cells, which are deficient in caspase 3, with RgA for 72 h resulted in poly(ADP-ribose) polymerase (PARP) and caspase 7 cleavage that was inhibited by cotreatment with the pancaspase inhibitor Z-VAD (Figure S10c), which indicative of apoptosis. We also determined the IC_{50} values for RgA against several human cancer cell lines using the alamar blue cell-proliferation assay. RgA dose-dependently inhibited proliferation of all the cancer cell lines tested, including the lung cancer cell line A549 and two breast cancer cell lines HCC1954 and MCF-7 (Figure 5a), with IC_{50} values ranging from 87 to 281 nM (Table S2), thus validating the antiproliferative activity of RgA.

Having demonstrated the antiproliferative and apoptosis-inducing effects of RgA in vitro, we proceeded to determine whether RgA was capable of blocking tumor xenograft growth in vivo. The fact that RgA inhibited multiple isoforms of GLUTs, including GLUT1, 3, and 4, raised the question of whether animals could tolerate RgA. since breast cancer cell lines are more sensitive to RgA than other cell lines (Figure 5a and Table S2), we assessed the anti-tumor activity of RgA against breast cancer in vivo. We selected two breast cancer cell lines for the xenograft experiment: MCF-7, an ER^+ $HER2^-$ line, and HCC1954, an ER^- $HER2^+$ breast line. NSG mice bearing MCF-7 tumors were given daily vehicle or RgA at a dose of 2 mg kg^{-1} for 38 days. Compared to vehicle control group, RgA treatment significantly delayed the xenograft growth of MCF-7 cells (Figure 5b), with tumor volume indexes on day 38 of 1.7 compared to 2.8 for the vehicle-treated group. In addition, RgA treatment significantly reduced the mean tumor weight from 454 mg (vehicle group) to 285 mg (treatment group; Figure S11a). Similarly, daily intraperitoneal injection of RgA at 2 mg kg^{-1} also effectively inhibited HCC1954 xenograft growth in nude

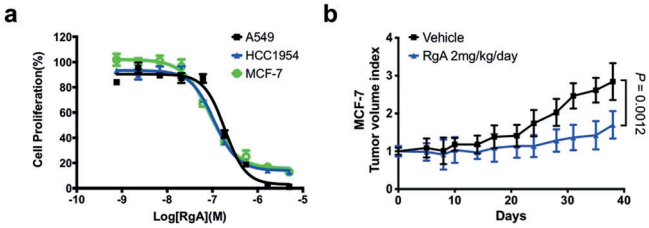

Figure 5. a) Inhibition of proliferation of A549, HCC1954, and MCF-7 cells by RgA. b) Analysis of tumor volume index following RgA or vehicle treatment in human breast cancer xenografts in mice. *P* value is from a two-sided student t-test.

mice (Figure S11c), with tumor volume indices on day 38 of 26.1 for vehicle treatment versus 13.0 for RgA treatment. Importantly, we did not observe any significant weight loss or other signs of adverse effects in animals receiving RgA during the course of the experiments (Figure S11), thus suggesting RgA at an efficacious dose was well tolerated in mice.

In conclusion, to facilitate the screening of the rapafucin libraries against new protein targets, we developed a microarray platform by immobilizing rapafucins on a chip surface. Using an optimized 3D microarray with a total of 3918 rapafucins on a single chip, we screened cell lysates containing stably expressed GLUT1. We identified several hits, two of which were confirmed as GLUT1 inhibitors in an orthogonal assay. The most potent inhibitor, named rapaglutin A (RgA), inhibited GLUT1 as well as GLUT3 and GLUT4 with an IC_{50} value of low nanomolar for GLUT1. We demonstrated that RgA inhibits glycolysis and ATP biogenesis, causing activation of AMPK, inhibition of mTOR, and induction of cell-cycle arrest and apoptosis. RgA also inhibited the growth of tumor xenografts of breast cancer cells in vivo without obvious side effects. Using the newly developed 3D rapafucin microarrays, we were able conduct a successful screen against a multi-pass transmembrane protein target for the first time. It will be interesting to screen the rapafucin microarrays against other types of multi-pass membrane proteins ranging from GPCRs to ion channels.

Acknowledgements

This work was made possible by the NIH Director's Pioneer Award, the Flight Attendant Medical Research Institute, a generous gift from Shengjun Yan and Hongju Mao and NCI (P30CA006973) (J.O.L.) and a Damon Runyon Postdoctoral Fellowship (H.P.).

Conflict of interest

Rapaglutin A has been patented by Johns Hopkins and licensed to Rapafusyn Pharmaceuticals. JOL is a cofounder and equity holder of Rapafusyn.

Keywords: antitumor compounds · drug discovery · GLUT1 · inhibitors · high-throughput screening

How to cite: *Angew. Chem. Int. Ed.* **2019**, *58*, 17158–17162
Angew. Chem. **2019**, *131*, 17318–17322

[1] O. Warburg, *Science* **1956**, *124*, 267–272.
[2] a) N. Hay, *Nat. Rev. Cancer* **2016**, *16*, 635–649; b) F. Schwartzenberg-Bar-Yoseph, M. Armoni, E. Karnieli, *Cancer Res.* **2004**, *64*, 2627–2633; c) J. Yun, C. Rago, I. Cheong, R. Pagliarini, P. Angenendt, H. Rajagopalan, K. Schmidt, J. K. Willson, S. Markowitz, S. Zhou, L. A. Diaz, Jr., V. E. Velculescu, C. Lengauer, K. W. Kinzler, B. Vogelstein, N. Papadppoulos, *Science* **2009**, *325*, 1555–1559; d) C. Chen, N. Pore, A. Behrooz, F. Ismail-Beigi, A. Maity, *J. Biol. Chem.* **2001**, *276*, 9519–9525.
[3] a) X. Cao, L. Fang, S. Gibbs, Y. Huang, Z. Dai, P. Wen, X. Zheng, W. Sadee, D. Sun, *Cancer Chemother. Pharmacol.* **2007**, *59*, 495–505; b) Y. Liu, Y. Cao, W. Zhang, S. Bergmeier, Y. Qian, H. Akbar, R. Colvin, J. Ding, L. Tong, S. Wu, J. Hines, X. Chen, *Mol. Cancer Ther.* **2012**, *11*, 1672–1682.
[4] Y. Qian, X. Wang, X. Chen, *World J. Transl. Med.* **2014**, *3*, 37–57.
[5] H. Siebeneicher, A. Cleve, H. Rehwinkel, R. Neuhaus, I. Heisler, T. Muller, M. Bauser, B. Buchmann, *ChemMedChem* **2016**, *11*, 2261–2271.
[6] a) H. Yang, D. G. Rudge, J. D. Koos, B. Vaidialingam, H. J. Yang, N. P. Pavletich, *Nature* **2013**, *497*, 217–223; b) J. P. Griffith, J. L. Kim, E. E. Kim, M. D. Sintchak, J. A. Thomson, M. J. Fitzgibbon, M. A. Fleming, P. R. Caron, K. Hsiao, M. A. Navia, *Cell* **1995**, *82*, 507–522; c) C. R. Kissinger, H. E. Parge, D. R. Knighton, C. T. Lewis, L. A. Pelletier, A. Tempczyk, V. J. Kalish, K. D. Tucker, R. E. Showalter, E. W. Moomaw, et al., *Nature* **1995**, *378*, 641–644; d) P. S. Marinec, L. Chen, K. J. Barr, M. W. Mutz, G. R. Crabtree, J. E. Gestwicki, *Proc. Natl. Acad. Sci. USA* **2009**, *106*, 1336–1341.
[7] Z. Guo, S. Y. Hong, J. Wang, S. Rehan, W. Liu, H. Peng, M. Das, W. Li, S. Bhat, B. Peiffer, B. R. Ullman, C. M. Tse, Z. Tarmakova, C. Schiene-Fischer, G. Fischer, I. Coe, V. O. Paavilainen, Z. Sun, J. O. Liu, *Nat. Chem.* **2019**, *11*, 254–263.
[8] a) Y. M. Foong, J. Fu, S. Q. Yao, M. Uttamchandani, *Curr. Opin. Chem. Biol.* **2012**, *16*, 234–242; b) J. A. Hong, D. V. Neel, D. Wassaf, F. Caballero, A. N. Koehler, *Curr. Opin. Chem. Biol.* **2014**, *18*, 21–28; c) M. Uttamchandani, S. Q. Yao, *Methods Mol. Biol.* **2017**, *1518*, 1–17.
[9] a) N. Kanoh, S. Kumashiro, S. Simizu, Y. Kondoh, S. Hatakeyama, H. Tashiro, H. Osada, *Angew. Chem. Int. Ed.* **2003**, *42*, 5584–5587; *Angew. Chem.* **2003**, *115*, 5742–5745; b) I. Miyazaki, S. Simizu, H. Okumura, S. Takagi, H. Osada, *Nat. Chem. Biol.* **2010**, *6*, 667–673.
[10] a) R. Barbey, L. Lavanant, D. Paripovic, N. Schuwer, C. Sugnaux, S. Tugulu, H. A. Klok, *Chem. Rev.* **2009**, *109*, 5437–5527; b) H. Ma, J. He, X. Liu, J. Gan, G. Jin, J. Zhou, *ACS Appl. Mater. Interfaces* **2010**, *2*, 3223–3230; c) J. O. Zoppe, N. C. Ataman, P. Mocny, J. Wang, J. Moraes, H. A. Klok, *Chem. Rev.* **2017**, *117*, 1105–1318; d) S. B. Lee, R. R. Koepsel, S. W. Morley, K. Matyjaszewski, Y. Sun, A. J. Russell, *Biomacromolecules* **2004**, *5*, 877–882.
[11] M. Kawatani, H. Osada, *MedChemComm* **2014**, *5*, 277–287.
[12] M. Mueckler, B. Thorens, *Mol. Aspects Med.* **2013**, *34*, 121–138.
[13] B. Hellwig, H. G. Joost, *Mol. Pharmacol.* **1991**, *40*, 383–389.
[14] B. E. Bierer, P. S. Mattila, R. F. Standaert, L. A. Herzenberg, S. J. Burakoff, G. Crabtree, S. L. Schreiber, *Proc. Natl. Acad. Sci. USA* **1990**, *87*, 9231–9235.
[15] X. Liu, Z. Ser, J. W. Locasale, *Anal. Chem.* **2014**, *86*, 2175–2184.
[16] S. A. Head, W. Q. Shi, E. J. Yang, B. A. Nacev, S. Y. Hong, K. K. Pasunooti, R. J. Li, J. S. Shim, J. O. Liu, *ACS Chem. Biol.* **2017**, *12*, 174–182.

Manuscript received: May 5, 2019
Revised manuscript received: September 3, 2019
Version of record online: October 31, 2019

